Simulation of millisecond catalytic partial oxidation of methane in a monolithic reactor for the production of hydrogen using finite element methods

by
Julie Flynn

Master in Engineering

Department of Chemical Engineering

McGill University

Montréal,Québec

2006-06-01

A THESIS SUBMITTED TO McGILL UNIVERSITY
IN PARTIAL FULFILLMENT OF THE REQUIREMENT OF THE DEGREE OF
MASTER IN ENGINEERING

Your file Votre référence
ISBN: 978-0-494-28595-4
Our file Notre référence
ISBN: 978-0-494-28595-4

DEDICATION

This document is dedicated to the graduate students of the McGill University.

ACKNOWLEDGMENTS

I am very grateful to my advisor, Professor Corey Leclerc, for his help, guidance and encouragements throughout the completion of this thesis. I learned a lot from his criticisms, many advises and suggestions.

I would like to thank Professors Coulombe, Rey and Berk for the courses that they taught in heat and mass transfer, computational methods and chemical reaction that helped me accomplish this work. I am also very grateful to many professors at the University Laval and Guadalajara University, which provided me a solid foundation in Chemical Engineering during my undergraduate studies.

I would also like to thank all members and staff of the department of chemical engineering that made the environment stimulating, and also friendly. And in particular, I cannot thank enough Akos Tota for the help, explanations, comments and suggestions that he provided.

I really enjoyed my graduate studies at McGill in English. Thanks to my friends and family, particularly my parents, who all supported me with encouragements during good as well as difficult times.

Finally, this research has been funded by Eugenie Ulmer Lamothe Fund.

ABSTRACT

Hydrogen can be the key solution of all our energy needs in the future and to face climate change while reducing greenhouse gases. Syngas, H_2 and CO, is industrially produced by steam reforming of methane. A potential alternative is the catalytic partial oxidation of methane. The process is fast, exothermic and auto-thermal.
A dual sequential bed catalyst is used, which makes use of a combustion catalyst followed by a reforming catalyst in order to carry out catalytic partial oxidation in two steps.
Numerical simulations using finite elements methods coupled with global kinetics are performed to have a better understanding of the transient process and the solid and gas temperature profiles in a catalyst. The results include temporal and spatial reactant conversion, product selectivity, and temperature profiles in the catalyst. Where possible simulation results are compared to experimental data.
The model shows high yields of hydrogen from methane and air which fits the experimental results in most of the cases. It also fits qualitatively the transient results. The influence of the kinetics was investigated and it is the principle limitation of the model which leads to a poor quantitative description.

RÉSUMÉ

L'hydrogène pourrait être la solution clé pour tous nos besoins énergétiques dans le futur et pour faire face aux changements climatiques tout en réduisant les gaz à effet de serre. Le gaz synthétique, H_2 et CO, est produit industriellement par le réformage à la vapeur du méthane. Une alternative potentielle est oxydation partielle catalytique du méthane. Le procédé est rapide, exothermique et autothermal.
Un lit catalytique séquentiel double est utilisé, il est composé d'un catalyseur sous forme monolithe pour la combustion suivi d'un catalyseur sous forme monolithe pour le reformage afin d'effectuer l'oxydation partielle catalytique en deux tapes.
Les simulations numériques employant la méthode des l'éléments finis couplé avec une cinétique globale sont effectués pour avoir une meilleure compréhension du processus en temps réel et les profiles de température du solide et de la phase gazeuse du catalyseur. Les résultats incluent la conversion des réactifs, la sélectivité des produits, et les profiles de température temporels et spatiaux dans le catalyseur. Quand cela est possible, les résultats des simulations sont comparés aux données expérimentales. Le modèle présente des rendements élevés pour la production d'hydrogène à partir du méthane et de l'air ce qui correspond aux résultats expérimentaux dans la plupart des cas. De plus, les résultats temporels sont également comparés qualitativement. L'influence de la cinétique a été étudiée et c'est la limitation principale du modèle ce qui mène à une pauvre description quantitative.

TABLE OF CONTENTS

LIST OF TABLES

LIST OF FIGURES

CHAPTER 1
Introduction

As the environmental impact of the combustion process has become more and more evident, the investigation of the production of clean energy has gained interest in society. The combustion of fossil fuels is a major source of greenhouse gas emission, and in Canada, the transportation sector is the single largest consumer source of greenhouse gas emission. The combustion of fossil fuels is a low efficiency, emission intensive process. The combustion of fuel also generates other toxic substances that are fouling our air, contributing to urban smog and threatening our health and the health of the planet.

The solution is a cleaner process. Hydrogen offers one potential answer to satisfying many of our energy needs while reducing carbon dioxide and greenhouse gas emissions. Hydrogen is a clean fuel with great potential as an alternative to combustion processes; particularly through its use in fuel cells which can generate electricity from hydrogen. Hydrogen is a much cleaner fuel than hydrocarbon feedstocks since the only tailpipe product from hydrogen fuel cells is water. The reaction occurring in fuel cells is exothermic with little emission of undesirable products. Moreover, fuel cells have a much higher energy efficiency compared to current combustion-based power plants. Fuel cells convert the chemical energy directly to electrical energy, without conversion of heat into mechanical work. An internal engine has a fuel efficiency around 12% in comparison of 50% efficiency for a fuel cell car.

In the automobile industry, fuel cells are one of the more attractive alternatives for the replacement of the internal combustion engine. The most promising fuel cells appears to be those equipped with proton exchange membranes (PEMFC) using hydrogen as the fuel. A major practical problem with such fuel cells is the storage of hydrogen, particularly since compression or liquefaction of hydrogen is very expensive. These problems associated with the production, distribution and on-board storage of the hydrogen gas have led to the consideration of compact and efficient devices to convert liquid carbon based fuels to hydrogen. Due to the presence of large natural gas reserves, research into the uses of methane, the principal component of natural gas has arisen. Methane can be converted into fuel, for instead hydrogen. Instead of storing hydrogen, a device called a reformer can be used to convert hydrocarbons into hydrogen. This device on board the vehicle operates like a small fuel processing plant producing hydrogen by partial oxidation.

Two principal methods for reforming fuel are steam reforming and catalytic partial oxidation. The most common method of producing hydrogen industrially is steam reforming of methane. The steam methane reforming process is a two-step process, where the methane, mixed with steam, is first passed over a nickel oxide catalyst at 900 °C and between 15-40 atmospheres. The reaction is:

$$CH_4 + H_2O \leftrightarrow 3H_2 + \mathrm{CO} \qquad \Delta\ \mathrm{H}_r = 205.9\ \mathrm{kJ/mol} \tag{1.1}$$

This reaction is endothermic; it requires external heat input, currently provided by burning natural gas or another fossil fuel. The tubular reactor is in a furnace.

The second step is a water-gas shift reaction, more steam is added and carbon monoxide is converted into carbon dioxide and more hydrogen is liberated from the steam by the following catalytic reaction:

$$CO + H_2O \leftrightarrow H_2 + CO_2 \qquad \Delta H_r = -42 \text{ kJ/mol} \tag{1.2}$$

Steam methane reforming is a slow process. Large amounts of steam are required, the residence time is on the order of 1 second and a large reactor, steam, and heat transfer equipment is needed. This process is limited by heat transfer and its large residence time which means, unfortunately, that this process cannot be scaled down. An essential characteristic for fuel cell applications is the need to reduce of the size of the reactor.

The second reforming method: catalytic partial oxidation, produces synthesis gas from methane and air. It is a exothermic reaction with a residence time on the order of the millisecond:

$$CH_4 + 1/2O_2 \rightarrow 2H_2 + CO \qquad \Delta H_r = -36 \text{ kJ/mol} \tag{1.3}$$

Catalytic partial oxidation has important thermodynamic advantages over steam reforming. It is exothermic, while steam reforming is highly endothermic. Thus, a partial oxidation reactor is more economical to heat, avoids the need for large amounts of expensive superheated steam and decreases the reactor size. Moreover, catalytic partial oxidation is a faster process than steam reforming; the time of reaction is in the order of a millisecond. Because of the small contact time, smaller reactors are used. In vehicle applications, a fast start-up is possible; you will be able to turn the key and the vehicle will start. The H_2/CO ratio produced in stoichiometric partial oxidation is approximately 2, and this ratio is ideal for downstream processes, in particular methanol synthesis. This avoids the need to remove valuable hydrogen, which is produced in excess in steam reforming. The product gases from methane partial oxidation can be extremely low in carbon dioxide content, but higher in carbon monoxide which must often be removed before synthesis gas can be used downstream, for example in fuel cells.

There are some disadvantages to the partial oxidation process. Because of high reactor temperature, the reactive mixture can lead to flames and explosions if operated in the flammability and explosive range. Also, local hot spots can cause material problems such as thermal stresses in the support and a decrease in catalytic activity due to catalyst sintering and volatilization.

Many studies have investigated the catalytic partial oxidation (CPO) of methane in short contact time reactors. The main goal has been to find optimal syngas yields and high conversion of CH_4. It was found that at millisecond residence times, CPO

is able to produce a high syngas selectivity of 90% with high methane conversion of 90% as reported by Hickman and Schmidt [1].

Hickman and Schmidt investigated the effect of space velocity and they showed a significant decrease in conversion and selectivity as the space velocity was raised between 10^5 to 10^6 h^{-1} [1]. In addition, Witt and Schmidt [2] also reported a decrease of methane conversion and syngas selectivity as space velocity was increased from 10^5 to $4x10^5$ h^{-1}. The space velocity is a significant limitation since it would be better to run as high a space velocity as possible to maximize syngas production. In the range GHSV investigated, the optimal GHSV is approximately 10^5 h^{-1} [1]. At this GHSV, the conversion and the selectivities are also optimal. They increase as GHSV increases until the critical point where the oxygen is forced through reactor too quickly to react.

Deutschmann and Schmidt reported the dependency of hydrogen and carbon monoxide selectivities on the methane to oxygen ratio. A good range for this ratio is between 1.7 and 2.1 to obtain desired CO and H_2 selectivities; a methane/oxygen ratio of about 1.8 was experimentally found to give the highest syngas yield in an autothermal, adiabatic reactor [3].

The effects of the ceramic supports have been reported by Bodke, Bharadwaj and Schmidt; when the catalyst porosity is decreased, the CO and H_2 yields increase [4]. This shows a mass transfer limitation since the rate is higher for catalysts with smaller pores.

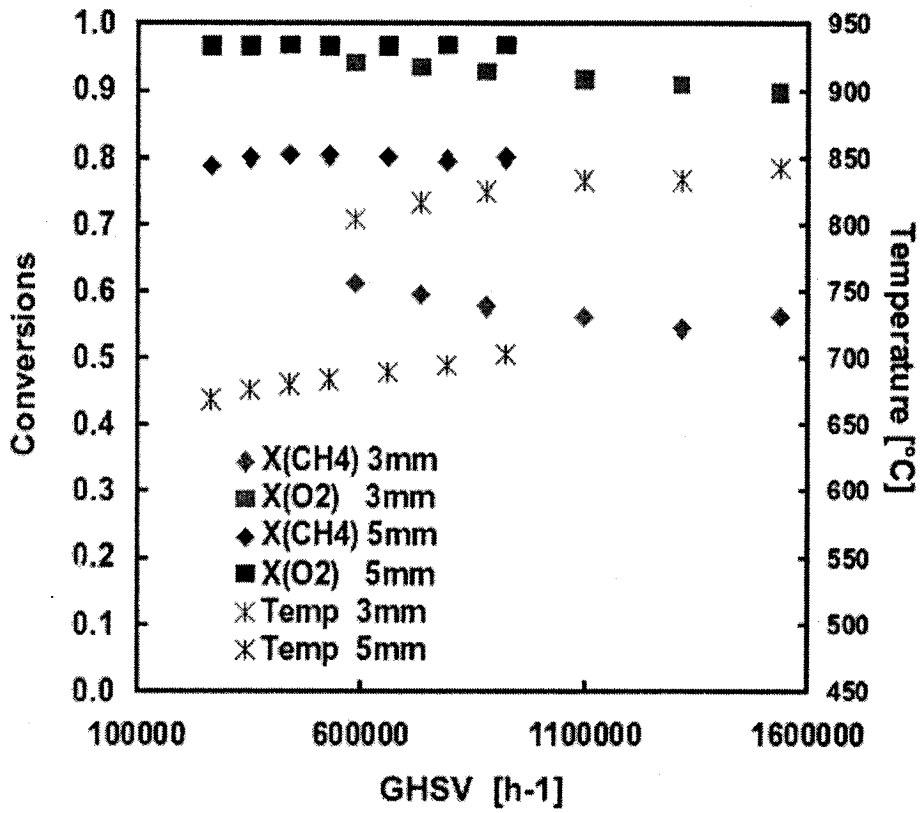

Figure 1–1: Experimental results for reactant conversions (oxygen and methane), and catalyst back face temperatures (secondary x-axis) for 3 and 5 mm rhodium catalyst at a ratio of 1.8 as a function of gas hour space velocity

In figure 1.1 show the results of the variation of catalyst length. As length of the catalyst was varied, conversion of oxygen goes to 96% for the 5 mm catalyst and slightly decreases from 94% to 90% for the 3 mm catalyst with an increase of GHSV. The conversion of methane is 80% for the 5 mm catalyst and varies between 61% to 54% for the 3 mm catalyst. The back face temperature of the 5 mm catalyst

increases from 669°C to 704°C with an increase of GHSV. For the 3 mm catalyst, it also increases with an increase of GHSV but from 804°C to 843°C. This represents a big step of 100°C for only 2 mm difference in catalyst length. This large difference in methane conversion of 20% can partially be explained by the different autothermal temperatures of reactions but also indicates the complexity of the system and the limitation of heat and mass transfer. These early experiments show that at the same experimental residence time , the conversion is different. For a constant GHSV, a plug flow model is not capable of predecting this change in reactant conversions, and cannot describe the behavior of the reactor.

Complex interaction between mass transfer, heat transfer, and chemistry occurs in catalytic partial oxidation as presented in different studies. Transport phenomena is important and it is influenced not only by the operating conditions, but also geometrical features, such as pore size or length-to-diameter ratio, the temperature profile and the steep gradients at the inlet. This is why, in this work, I will use modeling techniques validated with experimental data to better understand and predict the interaction of heat and mass transfer in catalytic partial oxidation. Modeling is used to investigate the behavior at dangerous operating conditions as the chemical reactions are potentially dangerous at high pressure and when performed without nitrogen; the mixture of pure oxygen and methane can be explosive. And to enlarge the understanding of the monolith interior, the presence of hot spots or intermediates will be investigated.

In other studies, computational tools for the numerical simulation of heterogeneous reactive flows were developed and there are two main approaches.

Hickman and Schmidt [1] performed the earliest simulation of a short contact time reactor system for conversion of methane to synthesis gas. This model, the plug flow model, is a tubular reactor operated continuously with a cylindrical geometry. The model can include the whole monolith or a single channel of the monolith as a plug flow tubular reactor (PFTR). This model describes an ideal one-dimensional flow pipe, in which no radial transport processes occur. The plug flow model using Chemkin solves the heterogeneous mechanism, and includes a full surface mechanism with 38 reactions, 7 gas phase species and 11 surface species, thermodynamic data and inlet conditions. In addition, it is assumed that temperature is uniform throughout the reactor and determined from a consistent heat balance with the reactor exit-product distribution. Therefore, a thermal energy equation is not needed and no mass transfer is involved. The plug flow model is not CPU intensive and it predicts CO and H_2 product selectivities that are consistent with the selectivities observed experimentally. However, there are some limitations.

Deutschmann and Schmidt [3] simulated the partial oxidation of methane to synthesis gas on rhodium. These authors were able to model the reactor in two dimensions, with full mass transport and momentum balances and heterogeneous reaction chemistry, using FLUENT coupled with external FORTRAN subroutines to simulate coverage-dependent surface reactions. In the gas phase, full heat transport was employed, but an isothermal condition was imposed on the wall where the temperature was chosen to be consistent with experimental observations. With only computational fluid dynamic software, as FLUENT, only basic surface kinetics, heat

CHAPTER 2
Objectives

The main objective of this work is to add what other models have left out or not coupled. This work includes the time dependency and the energy equation as these are the two mains important factors missing from previous models. This new model should incorporate correct results from the previous works while adding new understanding due to its increased complexity.

One of the main goals is to develop a 2-D model solving time dependency while coupling the energy equation, fluid mechanics and kinetics. The model will predict the gas phase species concentrations, the temperature profile of the gas and wall phase and the flow profile at steady state and during a transient.

This project objective is to investigate the effects of heat and mass transfer in the catalytic monolith of methane partial oxidation by exploring the connection between flow rate, catalyst bed length, and catalyst pore size. Of particular importance is the treatment of heat transfer between the solid and gaseous phase and conduction of heat in the catalytic monolith. Methane will be used since it is the simplest hydrocarbon fuel and does not exhibit gas phase chemistry during the partial oxidation process.

Therefore, by developing a model of the system, the number of experiments can be reduced greatly and scaling of the reactor system can be performed first in simulations before being carried out in the laboratory.

transfer, and fluid dynamics can be solved in order to describe the millisecond reaction in two dimensions. Although FLUENT is well equipped to solve fluid flow problems, it has limited capabilities to handle stiff chemistry, a large number of reactions, and it requires a lot of independent programming.

Every model has limitations. In the case of the two approaches explained above, the energy equation and the time dependency were not solved. Simulations need to show the complex interaction between heterogeneous chemistry and the reactor mass and heat transfer, especially at the catalyst entrance, where extremely rapid variations in temperature, velocity, and transport coefficients are observed.

As experimental results have shown, the total oxidation of methane takes place very quickly and occurs at the front of the monolith, generating very high temperatures. However, the thermocouple is only able to measure the back face temperature where the reaction has already been completed. This is why, it is important to create a model to determine the temperature profile inside the monolith and also the transient behavior The model may be used for an on-board reformer where the transient performance is much more important than an industrial hydrogen plan. In addition, the conditions at the start up and at steady state need to be as well considered for the temperature profile if future applications are to become commercially useful.

2.1 Challenges

One of the major challenges involved with this project is to first choose rational assumptions to formulate our model in order to be able to solve it in a reasonable amount of time. The second challenge is to apply a new computational tool which will include all the equations found in other models. The experimentation must be designed so that different parameters can be compared and data obtained from the different analyses can be related.

CHAPTER 3
Experimental

3.1 Experimental Conditions

The CH_4/Air mixture is fed to the reactor at room temperature and atmospheric pressure. The molar feed ratio, CH_4/O_2, is between 1.7 and 2.1. This range of ratios has been proven to be a good range to obtain high conversion and selectivity. The experimental set up is presented in figure 3.1. The reactor consists of a quartz tube about 20 cm long with an internal diameter of 18 mm. The catalyst is placed between two radiation shields, monoliths with pore densities of 45 pores per inch (ppi) and it is wrapped with a Fiberfrax paper. The monolith is wrapped to prevent gases from bypassing the catalyst, and the radiation shields are used to minimize radiant heat losses in the axial direction. Then the monolith is placed about 5 cm away from the reactor entry. At the beginning, the monolith is cold and it is heated by an external Bunsen burner until the reactor reaches the ignition point. Once the ignition point is reached, the burner is removed and the reactor is insulated with fiberglass insulation, Isofrax, to reduce the loss of heat from the wall of the reactor, to have adiabatic operation. The experiment is carried out at (i) auto-thermal conditions,since heat generated by the reaction is sufficient to sustain reaction and (ii) atmospheric pressure, as it has been shown to give high conversion and selectivities. High pressure catalytic partial oxidation at very short contact times has already been proven to be feasible and product selectivities do not change significantly as pressure rises [5].

3.2 Catalyst Preparation

The catalysts are prepared by the incipient wetness technique. The catalysts were supported on α-alumina cylindrical foam monoliths with pore densities of 80 ppi, diameter of 17 mm, and porosity of 0.83. It is performed in the lab from extruded, alumina foams coated with metal salts and subsequently calcined to remove the non-metallic portion of the salt. First, the alumina foam is washcoated using γ-Al_2O_3 diluted with distilled water. The solution is dripped onto the monolith, and then the monolith is air dried overnight. The desired loading for the wash coat is 5% by weight, but it can vary by $\pm$ 1%. After that, the metal precursors are diluted with distilled water, and the solution is dripped onto the wash-coated alumina monolith. After drying in air overnight, each catalyst is calcinated for about 6 hours at 600°C for the Ni, Pt and Rh to remove nitrate or chloride groups and leave only the metal on the support. The desired loading is also 5% by weight with some variations.

3.3 Instrumentation

The flow rates of methane and air are controlled by mass flow controllers (MFC); the dry air is controlled by a FC-261V Tylan thermal MFC and the methane is controlled by a FC-260V Tylan thermal MFC. The back face temperature is measured by a type-K thermocouple with an inconnel sheath of 0.20 inches diameter grounded and 18 inches long located between the catalyst and the downstream radiation shield. The entrance temperature is not measured, because it depends strongly on the position of the thermocouple, i.e. if it is in a pore or in contact with the monolith. The effluent gas is separated in a gas chromatograph, (GC) Agilent HP6890N, using two columns, a HP-PLOT Q capillary column is used to separate carbon dioxide from

the other gases and the other column, HP-PLOT molesieve 5A, is used to separate methane, oxygen, nitrogen and carbon monoxide. Balances on carbon atoms closed to within 5%. Helium is used as a carrier gas for detection on a thermal conductivity detector (TCD). The chromatograph is connected to a computer and the software ChemStation controls the GC. The diagram of the complete setting is presented in figure 3.2.

3.4 Start-up/Shutdown

Once the computer and the GC are on, the analysis method is loaded in the ChemStation and all the parameters are set-up. The thermocouple is introduced in the reactor and the reactor is fixed on its support. The mass flow controllers and the cylinder of dry air and methane are opened. The methane is turned on first then the air. The outlet pressure of the cylinders needs to be at 40 psi. The Bunsen burner is ignited and the reactor is heated for about 10-20 min depending on the catalyst in use. The catalyst ignition is associated with a jump in the back face temperature. The Bunsen burner is turned off and the reactor is insulated. Before the first sample is taken, the reactor needs to stabilize to a steady state temperature. Then the sample can be taken and analyzed by the GC. Only one sample at a time is analyzed and it requires 10-15 minutes. For each parameter of the experiment, three samples are analyzed. To shut down the reactor, the flow rate of air is turned off first then the methane is turned off, in order to avoid the formation of an explosive mixture.

3.5 GC Analysis

Once the sample is injected, the GC begins to analyze the sample. The time of the run is 15 min. When it is finished, the results are considered for their validity then entered into a spreadsheet, where the conversion and selectivity are calculated.

3.5.1 Conversion

The conversion of substance i is defined as the ratio of the amount reacted by the amount fed:

$$X_i = \frac{F_{i,in} - F_{i,out}}{F_{i,in}} \tag{3.1}$$

where $F_{i,in}$ is the flow of species i in the feed and $F_{i,out}$ is the flow of species i in the outlet.

3.5.2 Selectivity

The selectivity $S_{i,j}$ of species i with respect to atom j is the amount of that species in the product stream divided by the stoichiometric sum of all products (k) based on the j (carbon or hydrogen) atom:

$$S_{i,j} = \frac{\nu_{i,j} F_{i,out}}{\sum_k \nu_{k,j} F_{k,out}} \tag{3.2}$$

where $S_{i,j}$ is the selectivity of product i with respect to atom j, is the stoichiometric amount of j atoms in species i, and $F_{i,out}$ is the flow rate of product i. In this work, molecular hydrogen selectivity is based on hydrogen atoms and carbon monoxide selectivity is based on carbon atoms.

3.5.3 Gas Hourly Space Velocity

The gas hourly space velocity (GHSV) [h^{-1}] is calculated from the volumetric flow rate at standard conditions, temperature and pressure of 25 °C and 1 atm divided by the void volume of the catalyst:

$$GHSV = \frac{\upsilon_0}{\varepsilon V_{monolith}} \tag{3.3}$$

where υ_0 is the volumetric flow rate at standard conditions (STP), ε is the monolith void fraction, and $V_{monolith}$ is the volume of the monolith.

All reaction products, except for H_2O and H_2, were analyzed using the TCD on the HP-6890 GC. Due to the difference of the thermal conductivity between hydrogen (product) and helium (carrier gas) being small, the hydrogen concentration can not be detected accurately by means of a TCD. The oxygen balance is closed with the concentrations of water and the hydrogen atomic balance is closed with the concentrations of hydrogen. And the C-atom balance served as an internal standard, accounting for mole changes and it closed to within 5% in all cases. The nitrogen is used as the standard gas for the GC analysis.

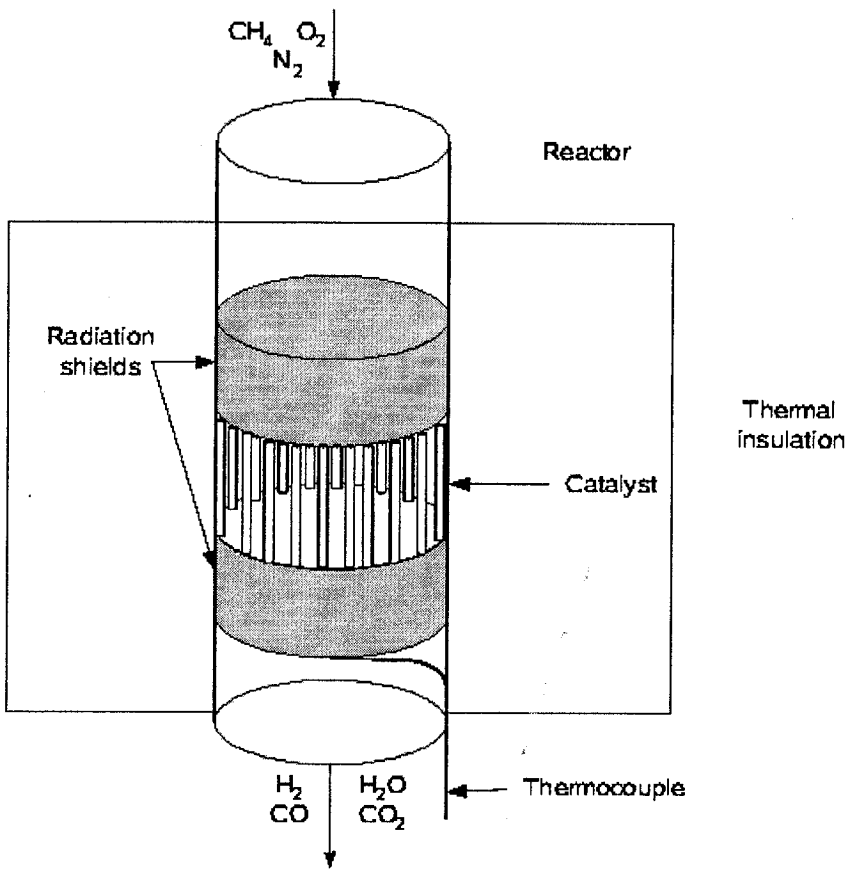

Figure 3–1: Diagram of the reactor

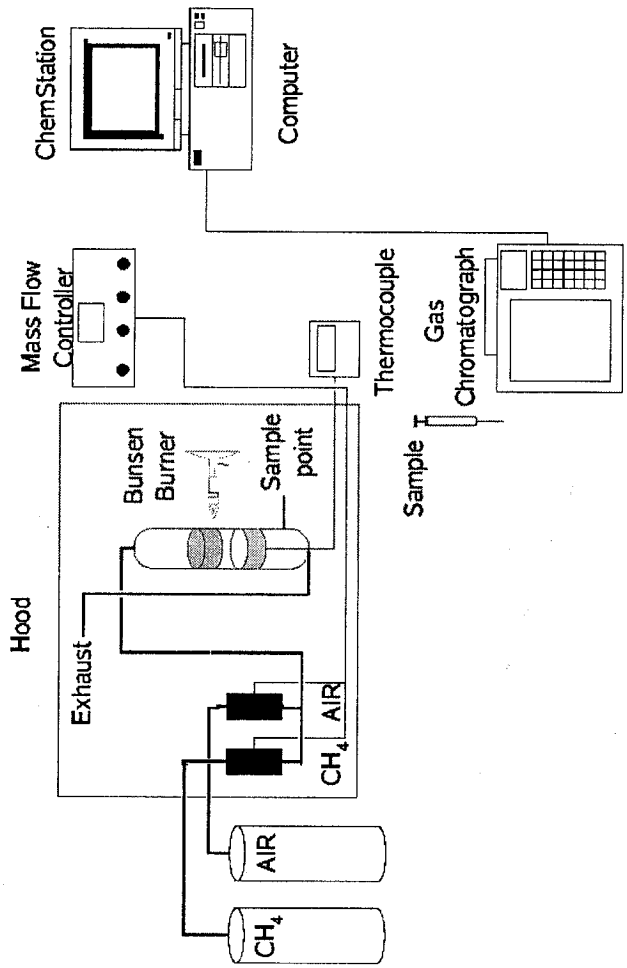

Figure 3–2: Diagram of the setting

CHAPTER 4
Modeling

The main purpose of this work is to develop an advanced time dependent, 2-D simulation model. This model should describe the temperature and species profiles within the catalyst using conservation equations for momentum, energy and mass with surface reactions. In a catalytic monolith, there are many physical and chemical processes that need to be coupled, such as the transport of momentum, energy, and chemical species in the axial and radial directions. The gas-surface interactions are significant; the chemical species can react either in the gas phase or on the catalytic channel's surface. The complexity of these problems make the development of such models complicated tasks.

This physical phenomena are heavily influenced by temperature and every variable, heat capacity, viscosity, thermal conductivity, diffusion, density, should be coupled to the temperature. One example of the importance of temperature is that of c_p, it has a considerable impact on heat generation and transfer. At the entrance, the temperature changes abruptly which causes rapid variation of transport coefficients and composition [6], also there are large gradients and the mass transfer at the surface is significant. Every variable is affected by this quick temperature change. This simple example alone illustrates well the complexity involved in the coupling of the conservation equations and the large temporal and spatial gradients that occur.

To reduce this complex system into a tractable problem,many assumptions must be made. In this transient 2-D model where the choice of consistent boundary conditions is essential, parameters were taken both from literature and from experimental results. The equations derived from the physical phenomenon discussed above are a set of partial differential equations that are strongly coupled, and highly nonlinear. They span a various length and time scales, for which a good example is that the residence time of the reactant is much smaller that the time scale for the temperature. Thus assumptions must be made for simplification. Using COMSOL[7], a commercial finite element software, the partial differential equations in the gas-phase and at the surface are solved while carefully considering the geometry and appropriate boundary conditions.

The significant difference between the model presented and those previously developed is the addition of the energy equation and time dependence. This addition of the time dependent energy equation allows us to investigate the development of temperature and species profiles in the catalyst as well as observe the time required to reach steady state hydrogen production. The work on catalytic partial oxidation reported in the literature was in most cases, carried out at atmospheric pressure. Development of high-pressure CPO reactors still requires considerable attention to ensure complete heterogeneous production of synthesis gas in the absence of homogeneous gas-phase reactions.

4.1 Model Equations

The basic equations are described using cylindrical spatial coordinates, as the whole catalyst can be reduced to a single channel. This single channel is represented

by a tubular geometry and easily modeled by an axisymmetric representation in cylindrical coordinates. This assumption simplifies the model and the symmetry plane is at r=0. The energy balance considers interphase heat transfer, conduction in the substrate and in the gas, as well as heat generation dues to chemical reaction. The species conservation equations account for convection, diffusion and production of species due to chemical reaction.

4.1.1 Mass and Momentum Conservation

The species conservation equations account for convection and radial diffusion. Since, there are seven gas species (CH_4, O_2, N_2, H_2, H_2O, CO, CO_2), seven conservation equations are needed to solve for gas phase species concentrations.

The diffusion and convection equation in the conservative formulation is:

$$\delta_{t,s}\frac{\partial c_i}{\partial t} + \bigtriangledown \cdot (-D_i \bigtriangledown c_i + c_i \mathbf{u}) = r_i \tag{4.1}$$

In cylindrical coordinates, this becomes:

$$\delta_{t,s}\frac{\partial c_i}{\partial t} - D_i(\frac{1}{r}\frac{\partial}{\partial r}(\frac{\partial c_i}{\partial r}) + \frac{\partial^2 c_i}{\partial z^2}) + \frac{\partial c_i}{\partial r}u + \frac{\partial c_i}{\partial z}v) = r_i \tag{4.2}$$

Where c_i denotes the concentration of species i, D_i denotes its diffusion coefficient, $\mathbf{u}$ the velocity vector, and r_i the reaction rate. In this model, the reaction rate

is equal to zero since the reactions take place at the surface boundary and not in the gas phase where the equation is solved.

The reaction term for the heterogeneous reaction is introduced as a boundary condition at the wall of the reactor. The rate of reaction must be equal to the flux of species perpendicular to the wall, and both terms are expressed mathematically below. In this expression, n represents the normal unit vector to the surface. The reaction rate, denoted r_i, is expressed as rate per unit surface (mole s^{-1} m^{-2}) and contains the kinetic expression for the reaction.

$$\nabla(-D_i \nabla c_i + c_i \mathbf{u})n + r_i = 0 \tag{4.3}$$

The momentum conservation equation for the reactor is obtained by solving either the Navier-Stokes equations or using the Poisseuille flow approximation. In the configuration, a zone before and after the reactive zone was added to fulfill the boundary conditions and the mass balances. Then a parabolic flow field is quickly established in the non-catalytic part. The assumption that the hydrodynamics are not dependent on the temperature simplified the simulation but leads to some difference between the simulation and experiments. The velocity in the entrance of the catalyst is affected by the change from the cold inlet feed to the hot catalytic wall. The density and the change of composition of the mixture also affected the flow field. With the assumptions that the gas has a uniform concentration and fully developed

flow where the velocity does not change along the flow axis. The analytical expression of the parabolic flow is descried by the Hangen-Poisseuille equation. Where the superficial flow rate is described as, $u_0 = \frac{v_0}{\Pi r_{gas}^2}$ and the laminar velocity form which is $u_z = 2u_0(1 - (\frac{r}{r_{gas}})^2)$. Alternatively, we could use the Navier-Stoke equations, which for a fluid flow are

$$\rho\frac{\partial u}{\partial t} - \eta \bigtriangledown^2 \mathbf{u} + \rho(u \cdot \bigtriangledown)\mathbf{u} + \bigtriangledown p = F \tag{4.4}$$

$$\bigtriangledown \cdot \mathbf{u} = 0 \tag{4.5}$$

The above two expressions represent the momentum balance and the equation of continuity for an incompressible flow, where η is the dynamic viscosity, ρ is the density, $\mathbf{u}$ is the velocity field , p is the pressure and F is a volume force field. It is important to note that solving the Navier-Stoke equations is computationally expensive.

4.1.2 Energy Conservation

The energy balance in the gas phase described conduction and convection of heat:

$$\rho c_{p,m} u\frac{\partial T}{\partial z} + \rho c_{p,m} v\frac{\partial T}{\partial r} = u\frac{\partial p}{\partial z} + \frac{1}{r}\frac{\partial}{\partial r}(\lambda r\frac{\partial T}{\partial r}) - \sum c_{p,k} j_{k,r}\frac{\partial T}{\partial r} - \sum h_k \omega_k W_k \tag{4.6}$$

The non-conservative formulation for conduction and convection in the gas phase is:

$$\delta_t s \rho c_p \frac{\partial T}{\partial t} + \nabla \cdot (-k \nabla T) = Q - \rho c_p u \cdot \nabla T \tag{4.7}$$

The heat capacity of the gas phase species is calculated as

$$c_p = \sum_{k=1}^{K} Y_k c_{p,k} \tag{4.8}$$

where $c_{p,k}$ is determined from the Stomate equation

$$c_{p,k} = A + BT + CT^2 + DT^3 + \frac{E}{T^2} \tag{4.9}$$

The energy balance in the wall only considers the conduction of the heat. The PDE formulation for the conduction of the heat in the wall is:

$$\delta_t s \rho c_p \frac{\partial T}{\partial t} - \nabla(k \cdot \nabla T) = Q \tag{4.10}$$

4.2 Reaction Kinetics

Globally, the formation of syngas from methane/oxygen mixtures on noble metal catalysts is characterized by the competition between a complete oxidation reaction:

$$CH_4 + 2\ O_2 \rightarrow 2H_2O + CO_2 \tag{4.11}$$

and a partial oxidation reaction:

$$CH_4 + 1/2\ O_2 \rightarrow 2H_2 + CO$$

(4.12)

The global reaction rate of partial oxidation cannot explain the production of CO_2 and H_2O. The indirect partial oxidation of methane is able to successfully described the production of all chemical species present, through the three following reactions.

Combustion

$$CH_4 + 2\ O_2 \rightarrow 2H_2O + CO_2 \qquad \Delta\ H_r = \text{-802.0 kJ/mol} \tag{4.13}$$

Reforming

$$CH_4 + H_2O \leftrightarrow 3H_2 + CO \qquad \Delta\ H_r = \text{+205.9 kJ/mol} \tag{4.14}$$

Water-gas shift

$$CO + H_2O \leftrightarrow H_2 + CO_2 \qquad \Delta\ H_r = \text{-42 kJ/mol} \tag{4.15}$$

Among the different catalysts used for catalytic partial oxidation, Rh is the best catalyst for CPO, it gives the highest yields and it is stable[8]. Dual bed catalysts formed of Pt and Ni is presently considered promising because of the use of cheaper metals. Moreover, there is no set of kinetic equations developed to describe the indirect methane partial oxidation on rhodium. Since the dual bed catalysts have been shown to give high hydrogen yields [9] and the kinetics for platinum and nickel

exist, they were used for this model. The sequential bed is composed of a platinum coated monolith for combustion followed by a nickel coated monolith for reforming.

Modeling catalytic reactions is complex and can be approached by several ways. The complexity of these reactions often leads to the use of global rate expressions and reactions rates. Reaction rates are based on the reactor specification and external conditions such as catalyst mass or volume, and reactor volume. They also depend on the temperature and gas phase concentrations. The most detailed and exact way to calculate heterogeneous reactions would be an elementary-kinetic approach, not many studies have been done on this. There also exists the possible use of a multi-step reaction mechanism consisting of a reduced set of selected elementary reactions, but the set can be excessively large. This represents a large amount of programming and different codes may need to be coupled, and the system of differential equation can be really stiff.

To describe the kinetics of the dual bed catalyst, the first part, the platinum catalyst, is described by the combustion of methane. For this reaction of methane on platinum, several Langmuir-Hinshelwood and Rideal-Eley models were developed and the best correlations were presented by Ma and Trimm [10]. The Langmuir-Hinshelwood mechanisms form an important class of reactions. These mechanisms consist of the following types of steps; adsorption from the gas-phase, desorption to the gas-phase, dissociation of molecules at the surface, and reactions between adsorbed molecules. These correlations were based on the adsorbed methane molecules

reacting with atomic oxygen. The kinetics parameters are presented in Table 4.1

$$r = \frac{k_1 K_1 \sqrt{K_2 P_{CH_4}} \sqrt{P_{O_2}}}{(1 + \sqrt{K_1 P_{CH_4}} + \sqrt{K_2 P_{O_2}})^2} \tag{4.16}$$

Table 4–1: Parameter estimates of combustion

Parameters	value	unit
A_1	0.365	mol/ m^2 s
Ea_1	34700	J/mol
K_1	$5.896e^{-2}$	kPa^{-1}
K_2	13.594	kPa^{-1}

For the second part, the model describes the reforming of methane. The description of the process cannot be based on a global reaction but by means of various partial reactions. It can be described by a set of three linearly independent reactions. However, the choice of the path may omit a dominant reaction in some part of the process in time or space or can alter the temperature profiles in some regions. The reforming is considered to take place through the following reactions: the steam reforming, the water gas shift, the CO_2 reforming , CO oxidation, methane reforming to CO_2 over a nickel catalyst.

One possible set of reaction for methane steam reforming over a nickel support catalyst was developed by Xu and Froment [11]. It can be represented by the following global reversible reactions:

Methane steam reforming

$$CH_4 + H_2O \rightarrow 3H_2 + CO \qquad r_1 = \frac{k_1}{P_{H_2}^{2.5}} (P_{CH_4} P_{H_2O} - \frac{P_{H_2}^3 P_{CO}}{K1}) / (DEN)^2 \tag{4.17}$$

Water gas shift

$$CO + H_2O \rightarrow H_2 + CO_2 \qquad r_2 = \frac{k_2}{P_{H_2}^{3.5}}(P_{CH_4}P_{H_2O}^2 - \frac{P_{H_2}^4 P_{CO_2}}{K2})/(DEN)^2 \tag{4.18}$$

Methane steam reforming to CO_2

$$CH_4 + 2H_2O \rightarrow 4H_2 + CO_2 \qquad r_3 = \frac{k_3}{P_{H_2}^{3.5}}(P_{CH_4}P_{H_2O}^2 - \frac{P_{H_2}^4 P_{CO_2}}{K3})/(DEN)^2 \tag{4.19}$$

where:

$$DEN = 1 + K_{CO}P_{CO} + K_{H2}P_{H2} + K_{CH_4}P_{CH_4} + K_{H_2O}P_{H_2O}/P_{H2} \tag{4.20}$$

The parameters estimates from the XF model are presented in Table 4.2 and Table 4.3, where the rate constants are from Arrhenius activation equation

$$k = AT^{\beta}exp(-\frac{E_a}{RT}) \tag{4.21}$$

Table 4–2: Parameter estimates of Xu and Froment model for $k_k = Aexp(-\frac{E_a}{RT})$

Reaction	k_k^o	unit	$E_{a,k}$ [J/mol]
k_1	$3.711e^{17}$	mol $Pa^{0.5}/kg_{cat}$ s	240100
k_2	5.43	mol/kg_{cat} s Pa	67130
k_3	$8.96e^{16}$	mol $Pa^{0.5}/kg_{cat}$ s	243900

Table 4–3: Parameter estimates of Xu and Froment model for $K_i = K_i^0 exp(-\frac{\Delta H_{ads,j}}{RT})$

Adsorption coefficient	K_i^o	unit	$\Delta H_{ads,j}$ [J/mol]
K_1	$4.707e^{22}$	Pa^2	+224000
K_2	$1.142e^{-2}$	-	-37300
K_3	$5.397e^{20}$	Pa	+186700
K_{CH_4}	$6.65e^{-9}$	Pa^{-1}	-38280
K_{CO}	$8.23e^{-10}$	Pa^{-1}	-70650
K_{H_2}	$6.12e^{-14}$	Pa^{-1}	-82900
K_{H_2O}	$1.77e^{5}$	-	+88680

A different set of equations to consider can be the methane steam reforming, the water gas shift and the CO_2 reforming reaction. The CO_2 reforming reaction over nickel was presented by Olsbye [12]:

$$CH_4 + CO_2 \rightarrow 2H_2 + 2CO \qquad r_{ref} = \frac{kP_{CH_4}P_{CO_2}}{(1 + K_1P_{CH_4} + K_2P_{CO})(1 + K_3P_{CO_2})} \quad (4.22)$$

Table 4–4: Parameter estimates of CO_2 reforming

	value	unit
k	4.45	mol/kg_{cat} s atm^2
K_1	0.52	atm^{-1}
K_2	10	atm^{-1}
K_3	27	atm^{-1}

4.3 Boundary Conditions

A standard boundary condition can be described by either a Dirichlet boundary condition or a Neumann boundary. The Dirichlet boundary condition is usually used at the inlet, where a chosen fixed value is giving for the variable under consideration.

The Neumann boundary condition is used at the centerline, the wall or the outlet, where a chosen flux is specified at the boundary.

4.3.1 Gas Phase

The principal boundary conditions used in this model are standard boundary conditions.

The boundary conditions applied to the conservation equations of momentum are for the inlet a constant velocity profile. The centerline is represented as the axial symmetry and the outlet is represented as the convective flux where it is a zero gradient. A zero velocity condition at the gas/surface boundary is applied.

The boundary conditions applied to the conservation equations of species are for the inlet the feed conditions $C_i = C_{i0}$. The inlet boundary conditions should be consistent also. It means that the sum of c_i should be c_0 on the inlet boundary. The centerline is represented as the axial symmetry and the outlet is represented as the convective flux where it is a zero flux. The wall boundary condition is represented as the flux of the species $n \cdot (-D_i \bigtriangledown c_i + cu) = -r$

The boundary conditions used for the conservation equation of energy are for the inlet feed temperature. The centerline is represented as the axial symmetry and the outlet is represented as the convective flux where it is a zero flux. The wall boundary condition is represent as the heat flux of the species $n \cdot (k \bigtriangledown T) = Q$

4.3.2 Wall

The boundary conditions used for the conservation equation of energy at the inlet and outlet is insulation. The wall/gas boundary condition is represented as

the heat released by reactions, which contributes to the energy balance at the gas-surface interface. Diffusive and convective fluxes in the gas phase are balanced by the chemical releases at the surface.

4.4 Important Model Considerations

The two-dimensional axisymmetric model is used and the reactor is described by two-dimensional conservation equations using a cylindrical geometry. Because of reactor symmetry the differential equations will only be solved for half the reactor. A single catalyst channel is modeled as a tubular reactor with constant radius and constant wall thickness. The characteristic pore diameter is 0.21 mm for an 80 ppi support, while the length of the catalytic part of the reactor is 3, 5 or 10 mm. In this diameter, the flow field is always laminar with a Reynolds number around 20. The flow erters the computational domain (z = -1 mm, r) at a known velocity, composition and temperature. The catalytic walls are conducting with a thermal conductivity of 12.6 W/m K which corresponds to aluminum oxide.

One feature of the computational domain is that both gas phase and the wall are spatially discretized. To avoid scaling difficulties, a map mesh is used and is divergent free so the continuity equation is better fulfilled than with triangular mesh. The total number of elements used is 6000, and the mesh quality is 0.80. The solution is assured to be mesh independent.

4.5 Software and Computer

COMSOL is a software for modeling and solving problems made up of partial differential equations. With this software, multiphysics models can be solved by coupling various physical phenomena simultaneously. COMSOL uses the finite element

method to solve systems of PDE s with error control applicable with different numerical solvers. During simulation, absolute and relative errors of 10^{-4} and 10^{-5} were used to ensure a better accuracy between each time step. The computer used for the simulations is a desktop computer with an Athlon FX-57 64 bit processor, A8N SLI Deluxe motherboard, XFX GF 6200 Graphic card, 2 GB RAM and Suse 9.3 operating system. The runtime for the standard simulation is approximately 1595 seconds.

4.6 Model Assumptions

The model was developed using the assumptions mentioned before and the following assumptions:

Ideal gas is assumed as temperature and pressure are low enough.

$$c_i = \sum_{i=1}^{n} p/RT \tag{4.23}$$

The real reaction is occurring in a monolith, where the monolith consists of a large number of tortuous channels. However, the simulation of the whole catalyst is reduced to the simulation of a single channel, and it is assumed that all channels in the monolith are identical and behave similarly. The model can then be reduced to a 2D transient axial symmetry.

A laminar flow is assumed. This assumption leads to the use of the Poisseuille flow and much less computation time is required. Moreover, the hydrodynamics does not depend on the gas composition and the temperature. The inlet profile of velocity is assumed uniform and constant.

Radiative heat transfer is not considered as the reactor is insulated. Since the temperatures inside the catalyst are below 1200 K and the operating pressure is near atmospheric pressure, the homogeneous reactions are not considered. It is generally assumed that the influence of gas phase chemistry on the overall conversion can be neglected at atmospheric pressure because the residence time is on the order of one millisecond, a time which is too short to ignite the mixture homogeneously.(8)

The number of active sites is assumed constant. Chemical reactions occur only on the external surface of the catalytic wall. The influence of pore diffusion in the washcoat is neglected. The inlet profiles of velocity, gas temperature, and species mass fractions are assumed to be uniform.

Table 4–5: Operating conditions for simulations

	value	unit
Reactor length	l	0.01 m
Channel radius	r_{gas}	$1e^{-4}$m
Wall radius	r_{wall}	$1e^{-5}$m
Intel temperature	T_0	500 °C
Feed composition		
methane	cCH_{40}	
oxygen	cO_{20}	
nitrogen	c_i	
Intel flow rate	v_0	$2e^{-8}$ m^3/s
Thermal conductivity	λ	12.6 W/m K

4.7 Validation

The model is verified by a comparison of the steady-state solution and the results obtained by Tong et al. [9]. The computed concentrations and temperature at the exit are compared with the experimental results. No validation is possible for the

inside of the monolith as the temperature, concentrations and intermediates cannot be measured. Attempts at capturing spatial profiles have been done by performing variable bed length experiments to determine the content of components. These samples were taken and compared to the simulation results. The transient solution is verified by a comparison of the experimental results presented by Williams [13]. The computed transient concentrations and temperatures are compared only qualitatively with the Williams results since the reactor conditions are different.

CHAPTER 5
Results

5.1 Time Dependency

The catalytic partial oxidation of methane was performed over a dual catalyst bed, where the first catalyst, oxidation section, was used to convert all the oxygen and partially converted methane to water and carbon dioxide, subsequently the remaining methane and products are converted in the second catalyst, reforming section. In the oxidation section, the gas temperature rapidly increases to the maximum temperature and in the reforming section while methane is converted with water and carbon dioxide. The dual bed was composed of a 5 mm Pt and a 5 mm Ni. But also in a mixed bed Pt/Ni was simulated as a comparison tool. Mixed bed catalysts have been done experimentally by Trimm et al [14] and have shown high methane conversion. Simulations were carried out at atmospheric pressure, inlet velocity was 0.63 m/s and the inlet temperature was 500°C with methane to oxygen ratio of 2.

5.1.1 Temperature Profile

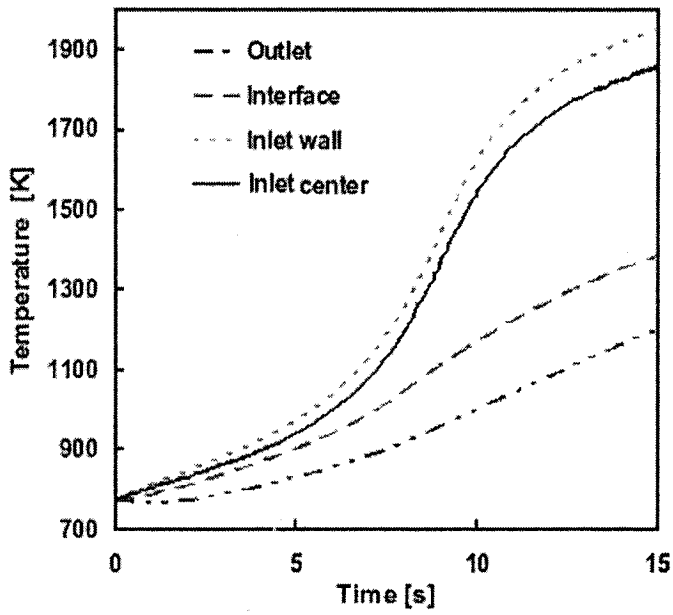

Figure 5–1: Back face temperature, interface temperature and entrance temperature in a dual sequential bed as a function of time

Figure 5.1 shows a plot of the back face temperature, the center-line temperature and the entrance temperature in a dual sequential bed. While gas and solid phase catalyst entrance temperatures are slightly different because the important amount of heat produces by combustion at the surface ,they are identical at the catalyst exit and the interface. Again, the temperature needs about 5 or 6 seconds before beginning to increase more rapidly. No hot spots are observed.

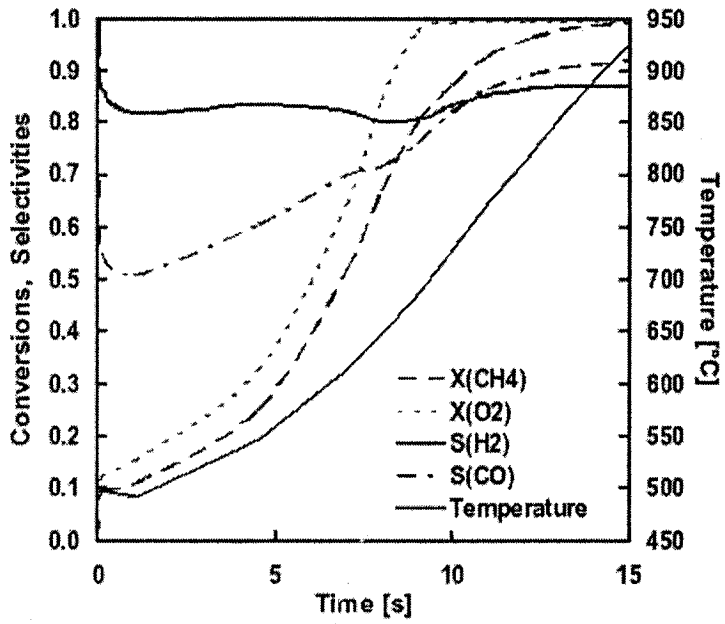

Figure 5–2: Reactant conversions of a dual sequential bed (oxygen and methane), product selectivities (hydrogen and carbon monoxide), and catalyst back face temperatures (secondary x-axis) as a function of time

Figure 5.2 shows a plot of back face temperature, methane conversion, oxygen conversion, hydrogen selectivity and carbon monoxide selectivity of a dual sequential bed. The back face temperature decreases initially in the first second due to the time required to heat up and start. Then it increases linearly to reach a value of 925°C.

The typical inlet gas temperature used in simulations is T_0= 500°C. If this inlet temperature is too low, the reaction takes a longer time to start because it needs to preheat the monolith or the reactions will not start. In previous investigations, it was found for a foam monolith that the catalytic light off temperature was T < 400

°C [15]. The initial temperature needs to be sufficiently high to ignite the reaction. Once the reaction is started, the entrance temperature increases to 1000 °C within the first 0.5 mm of the catalyst in only 3 or 4 seconds. The simulation results show that the catalyst temperature decreases initially, as the reforming rates of the model are significantly higher and just after the methane oxidation starts. After that minimum value is passed, the heat produced during combustion is sufficiently high to cause an increase of the temperature.

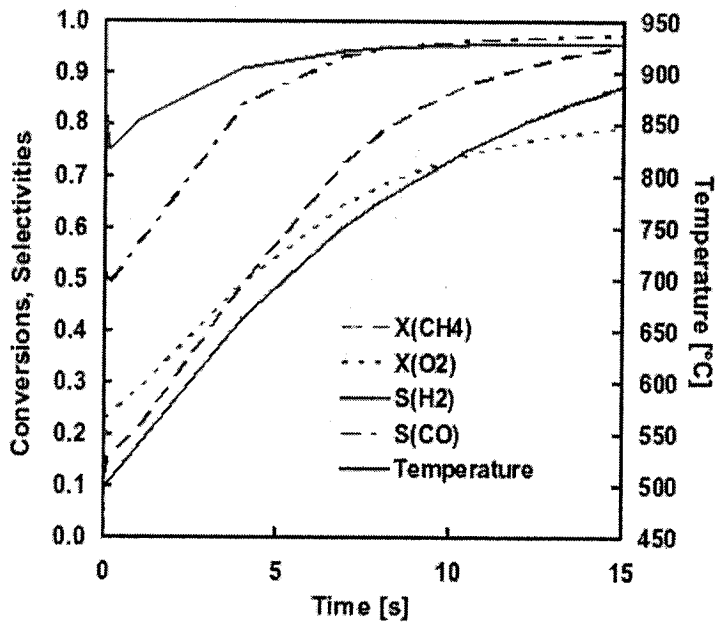

Figure 5–3: Reactant conversions of a mixed catalyst (oxygen and methane), product selectivities (hydrogen and carbon monoxide), and catalyst back face temperatures (secondary x-axis) as a function of time

Figure 5.3 shows a plot of back face temperature, methane conversion, oxygen conversion, hydrogen selectivity and carbon monoxide selectivity of a mixed catalyst composed of Pt/Ni for simulation carried out at 0.63 m/s with a methane to air ratio of 2. The back face temperature increases linearly to a value of 880°C.

5.1.2 Concentration Profile

The concentration profile of reactants (CH_4, O_2) and all products (H_2, CO, H_2O, CO_2) were calculated at the exit of the reactor. After t= 0s, the combustion mixture, oxygen and methane decrease toward zero, whereas hydrogen and carbon monoxide production begins to increase, and flow rates start to rapidly increase around 5 seconds. Hydrogen, carbon monoxide, and methane reach their steady-state values within 15 seconds. Figure 5.2 ,for the dual bed shows the conversion of methane takes some time to increase and then increases abruptly around 5 seconds until it reaches a constant value of almost 100% in 11 to 12 seconds .The conversion of oxygen follows the same trend as the methane conversion but increases even more abruptly and also reaches a constant value of 100% faster in only 8 seconds. The selectivity of hydrogen first starts at 100% and decreases rapidly to a value around 82%. It stabilizes after 10 seconds to a value of 86%. The selectivity of carbon monoxide decreases initially but then increases and reached a constant value of 92% in about 11 to 12 seconds. Figure 5.3, for the mixed bed, the conversion of methane increases linearly until it reaches a constant value of 95% in about 12 seconds . The conversion of oxygen follows the same trend as the methane conversion but increases less abruptly and reached a constant value of 78% in 11 seconds. The selectivity of hydrogen first starts at 100% and decreases rapidly to a value around 75%. It

stabilizes after 6 seconds to a value of to 95%. The selectivity of carbon monoxide decreases initially to 49% and increases to a constant value of 97% in about the same time as the selectivity of hydrogen. Comparison of figures 5.2 and 5.3 show that the carbon monoxide selectivity reached a stable value of 90% in 10 to 15 seconds in the sequential bed, in the mixed catalyst the value reached 95% in a lower time and the curve is smoother. Hydrogen selectivity reached a stable value of 85% rapidly in the sequential bed, in the mixed catalyst the value reached 95% in 5 seconds and again the curve seems smoother.

The calculated concentration profiles show that the performance of the catalytic monolithic reactor is influenced by the temperature, the length of the combustion, the inlet composition and velocity. CO and H_2 concentration profiles on one hand, and CO_2 and H_2O concentration profiles on the other show very similar curves. Syngas concentrations show a strong increase in the reforming catalyst bed. The concentration of methane in the channel is along the axis and it has a parabolic shape due to the flow.

5.2 Steady State

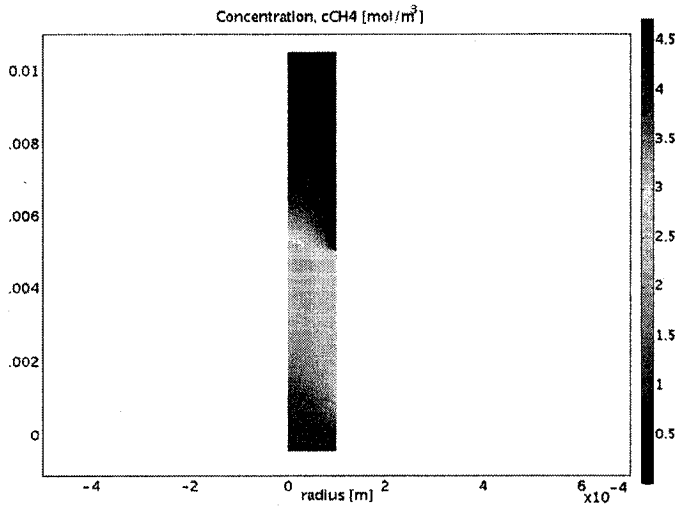

Figure 5–4: Methane concentration in a dual sequential bed

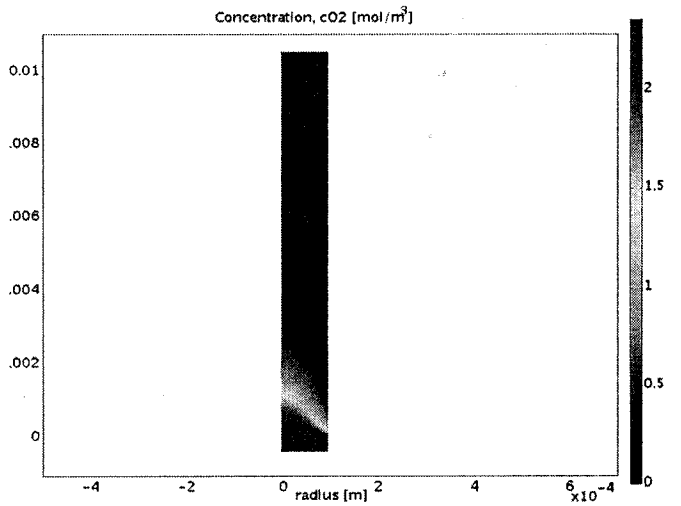

Figure 5–5: Oxygen concentration in a dual sequential bed

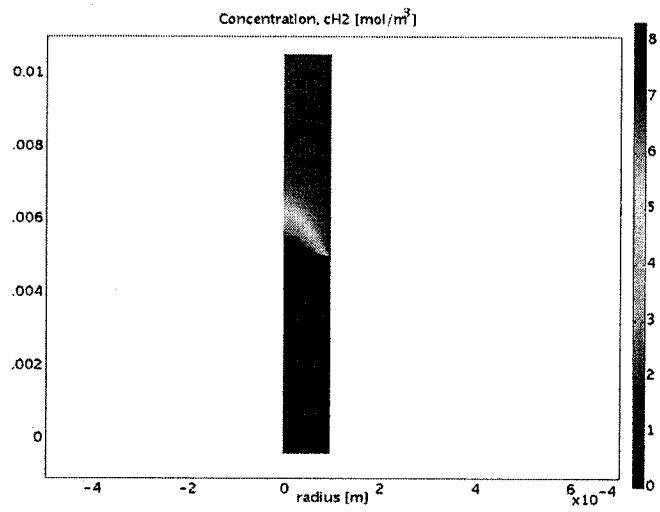

Figure 5–6: Hydrogen concentration in a dual sequential bed

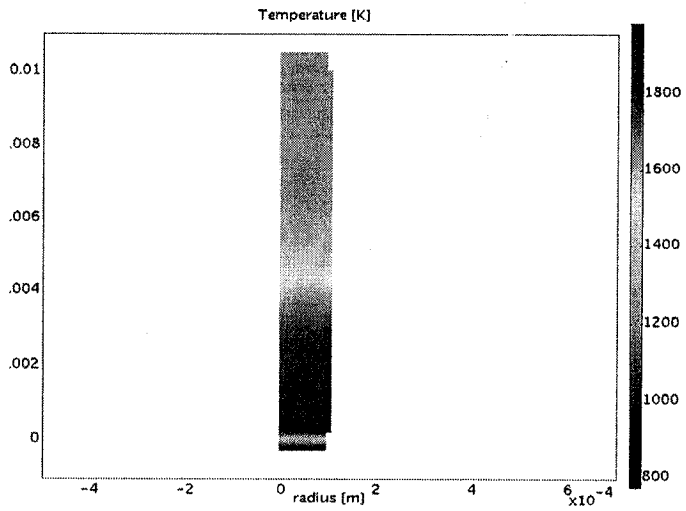

Figure 5–7: Temperature in a dual sequential bed

Figures 5.4 to 5.7 show the contour plot of methane, oxygen and hydrogen concentration and the temperature profile inside the monolith for a dual sequential bed composed of a combustion and a reforming catalyst. The methane is quickly used in the combustion part with all the oxygen and the remaining methane is used with the carbon dioxide and the water produced in the first part. The oxygen concentration is reacting quickly in the two first millimeters, as found experimentally. The hydrogen is only produced in the reforming part. The temperature profile shows a very hot part at the beginning of the catalyst where the combustion occurs and afterward the temperature cools off.

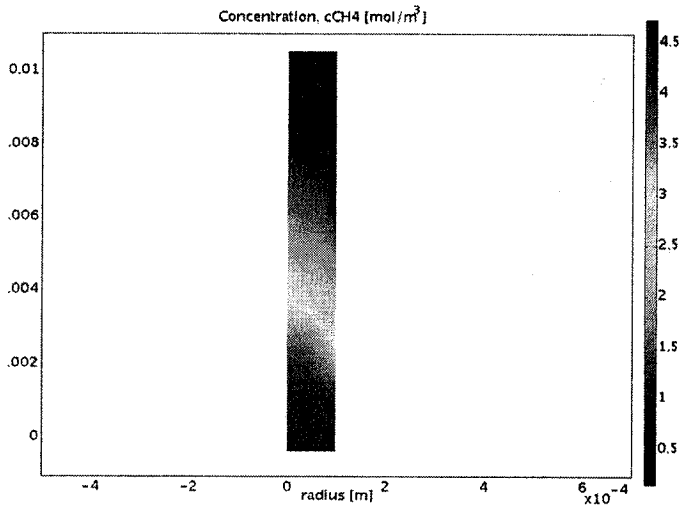

Figure 5–8: Methane concentration in a mixed bed

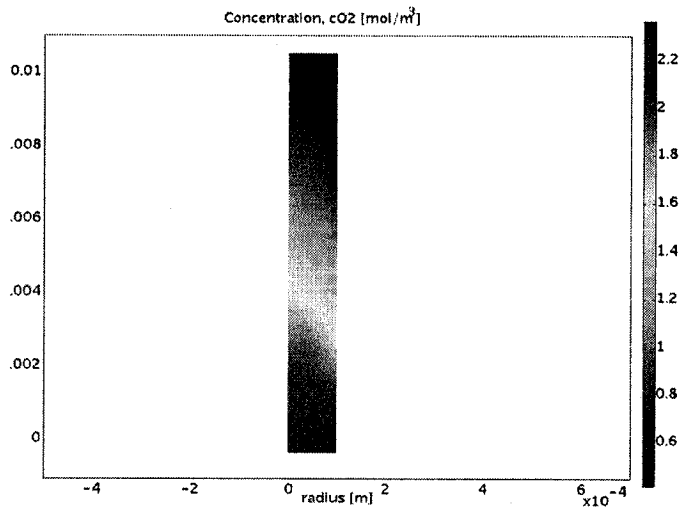

Figure 5–9: Oxygen concentration in a mixed bed

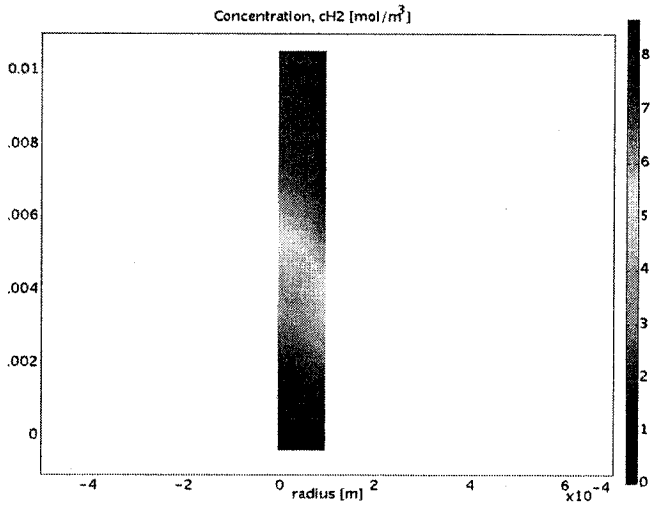

Figure 5–10: Hydrogen concentration in a mixed bed

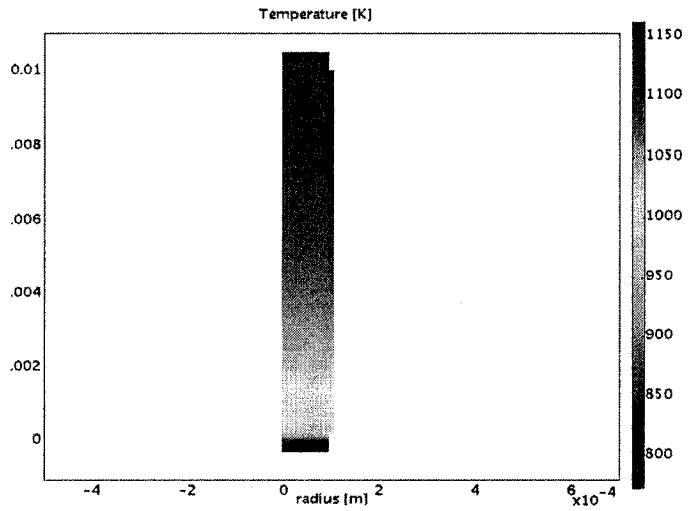

Figure 5–11: Temperature in a mixed bed

Figures 5.8 to 5.11 show the contour plot of methane, oxygen and hydrogen concentration and the temperature profile inside the monolith for a mixed bed where the nickel and platinum are mixed in the same catalyst. The methane is uniformly used. The oxygen concentration profile is also uniform, only half of the oxygen is converted after 5 mm which is not observed experimentally. The conversion of oxygen is slow. The hydrogen is also uniform. The temperature profile is the reverse of what experimentally is observed. The front face is cooler and the back face is warmer.

5.3 Experimental versus Simulation Results

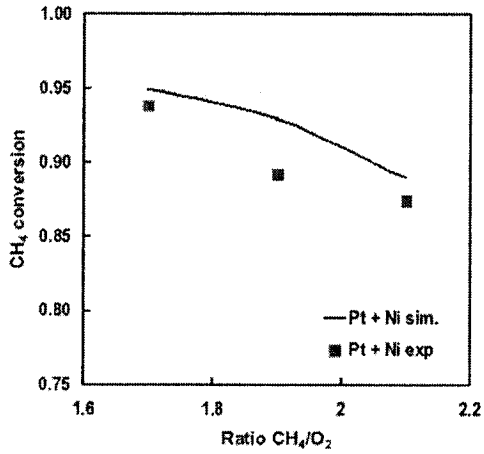

Figure 5–12: Methane concentration in a mixed bed as a function of the methane/oxygen ratio

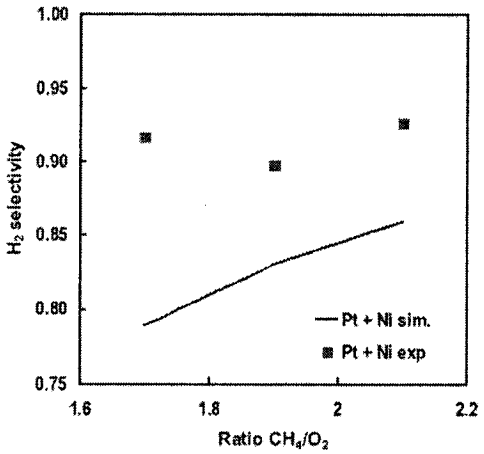

Figure 5–13: Hydrogen as a function of the methane/oxygen ratio

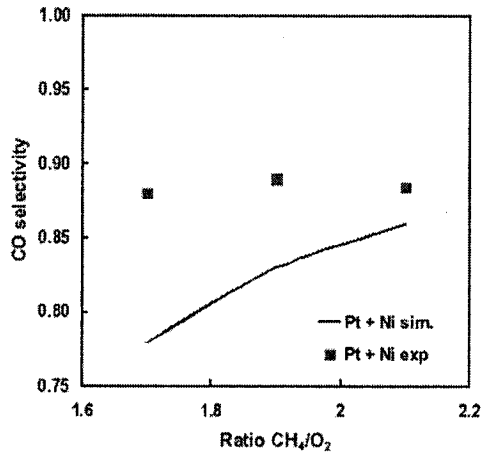

Figure 5–14: Carbon monoxide selectivity as a function of the methane/oxygen ratio

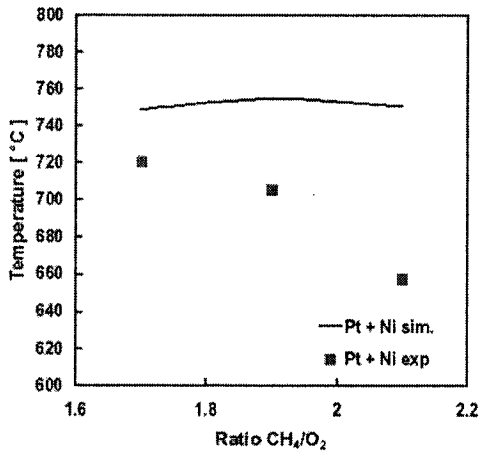

Figure 5–15: Temperature as a function of the methane/oxygen

In figures 5.12 to 5.15, lines represent simulations and symbols experiments for different ratios. The conversion of methane also decreases as the methane to

oxygen ratio increases for both simulation and experiments. The experiments show a decrease of 6% from 94% to 88% and the simulation shows the same 6% but from 95% to 89%. The experimental selectivity of hydrogen and carbon monoxide show almost no change over the feed ratios but show the simulation predicts a more noticable change in hydrogen and carbon monoxide selectivities. The experimental back face temperature shows a decrease from 720°C to 660°C as the feed ratio increases from 1.7 to 2.1, and the simulated back face temperature remained at a constant value of 750°C in the same range of feed ratio.

CHAPTER 6
Discussion

6.1 Kinetics

The choice of the kinetic equations affected the model. The first limitation of the dual bed model is the absence of steam reforming on the platinum catalyst. In the numerical simulation, the rate equation of steam reforming on platinum is not available in the literature and was not applied. In contrast, experimentally on the platinum catalyst, combustion and steam reforming of methane both occur.

The second limitation is the applied kinetics of steam reforming from Xu and Froment model. This set of equation leads to a non convergence of the simulation, a negative value of the water concentration occurs. The rate of reaction has in the denominator hydrogen and water, but the system does not contain hydrogen or water in the inlet feed, so the model was made applicable by adding a very small value to every concentration. This term may influence the rate which directly influences the heat-generation, the temperature profile as well as the conversion and selectivity. This can be the cause of higher calculated temperature comapre to the experimental results obtain in [9].

The third limitation is the applied kinetics of combustion on platinum from Trimm and Lam [10]. The combustion kinetics were estimated for a fixed catalyst temperature of 830K. The kinetic rate expressions were developed from different types of reactors, they may include mass transfer in the reaction parameters which

may be responsible for much of the difference between the model with the experimental results.

The comparison between two different configurations, dual bed catalyst and mixed catalyst, was made to show the competition between the different kinetics. This comparison proves that the steam reforming is faster and in the mixed bed the combustion of methane is in competition, this is why the oxygen is not fully converted..

6.2 Time Dependency

6.2.1 Temperature

Temperature is one of the most important parameters as it determines the conversion and the selectivity. It is also essential to understand the heat transfer between the gas and the solid phase, and the effects on the reactions. The experimental results can only measure the back face temperature. No data are available for the inside temperature and to provide explanation of the temperature profile of the whole monolith, this is why, numerical simulation is used.

Experimentally, the total oxidation of methane takes place very quickly and occurs at the front of the monolith generating very high temperatures. A look at the catalyst during the reaction shows a glowing orange ring at the entrance of the monolith. Catalyst exit temperatures give good agreement with the experimental data. As the experimental results show, the bed always needs to be preheated to light off the reaction. In the simulation as well, the initial temperature needs to be high enough to have a quiet start up.

However, catalyst entrance temperatures were not measured experimentally and simulation results therefore are not validated against this variable. But the temperature is increased slower than expected, which can lead to the conclusion that the simulated combustion reaction is too slow. In the model, the interface in the dual sequential bed may not be described adequately. The interaction between the two monoliths is much more complex with the heat and mass tranfer , the contact between them and the possible change in composition. Qualitative differences between experiment and simulation suggest that some features of the monolithic reactor are not modeled adequately yet. At the entrance, the mixture is affected by the hot temperature of the catalytic part and the change in thermal conductivity of the mixture help the increase of the gas temperature. It as been shown that the heat capacity as a strong effect on the catalytic temperature [6]. A possibility to improve the temperature profile if the heat transfer module is available, it is the use of the highly conductive boundary condition. Some others studies also included a term for the radiation, it may have some impacts on the performance of the reactor.

6.2.2 Conversions and Selectivities

The selectivities and conversion calculated by numerical simulations don't have any experimental references in transient state and cannot be quantitatively validated. The selectivity can be high even if almost nothing is produced. The only comparison possible is with the transient experiments of Williams [13] and even so, those experiments were in different conditions than the experimental and numerical simulations of this present work. Willams used different reactants (CH_4, O_2 and Ar) and a spark

generator to ignite the combustion feed, and the reactor was preheated and then the fuel flowed to the stoichiometric ratio of partial oxidation.

The simulated conversion of methane and oxygen seems to have a reasonable velocity, but the conversion of oxygen should be much faster than the conversion of methane. This shows that the combustion kinetics are too slow. The selectivity of hydrogen and carbon monoxide are higher than expected; this also indicates that the reforming is fast. The drastic decrease changes in the first few hundred milliseconds may be a numerical error or the adsorption of the reactants , but it is nearly impossible to measure.Concentration curves thus generally suggest that a major part of the reaction takes place in first part of the catalyst, where steep concentrations profiles are observed. The fact that CO_2 concentration is low, indicates that the CO_2 reforming is not as pronounced as steam reforming. Time-dependent concentrations measured at the reactor exit show a good qualitative agreement with experiments and suggest that global kinetics once adjusted can be modeled correctly.

6.3 Steady State

6.3.1 Temperature

The bed temperature is slightly higher in the dual bed then the one mixed in time but it is higher at the beginning in the mixed one as all the catalyst can produce heat from the combustion reaction. The temperature profile found shows a very high temperature at the entrance which may be too high. This can be due to the thermal conductivity of the catalytic wall which is much larger than the one in the gas phase. And the thermal conductivity of the gas phase was modeled as an expression depending on temperature for air. Also the temperature profile is very

sensible to the size of the catalytic wall. The preheat inlet flow could give a higher temperature.

Generally, the simulations give higher selectivities and conversions then the experiment. Radial heat loss occurs through the insulation which decreases the experimental temperature in comparison of the simulation ,where no heat loss occurs. Also the measured back face temperature is $\pm 50^{o}$C which depends on whether the thermocouple is touching the monolith or it is in front of a pore.

6.3.2 Concentration

The dual sequential bed model gives a good global representation. If the reforming reaction rate on platinum was known, it would be expected to give better fit with the experimental data. The mixed bed really shows the competition in the use of the methane with oxygen, water and carbon dioxide. It also shows that water and carbon dioxide are the fastest reactions and the oxygen is the slowest, but that the oxygen reaction is still needed to produce water and carbon dioxide. The temperature profile can be explained by the concentration profile of oxygen. In the first part, the reforming is much more prevalent, but after combustion starts, it enhances the production of heat in the monolith.But this is not realistic as the reverse would be expected.

6.4 Future works

Different parameters are not considered in the present work, but here are some possibilities that can improve the model. One possibility is the use the Maxwell-Stefan diffusion module for multicomponentflows. The diffusion is an important parameter as it is known that the diffusion coefficient of hydrogen is higher compared

to carbon monoxide. The use of numerical diffusion (artificial diffusion), in this case, the streamline diffusion, where an extra diffusion term depending on the size of the mesh is add locally, smooth the instabilities and help greatly the convergence. An other good way to capture sharp fronts and localized gradients is through local mesh refinement and specialized formulation such as Petrov-Galerkin. The developed of a model with a step mechanism will requires the use of the weak boundary form to related the gas phase species with the reactions occuring on the surface.

CHAPTER 7
Conclusion

The environmental benefits of fuel cells are some of the main motivating forces in their development. These benefits include the zero- or near-zero-emission criteria of pollutants (NOx, SOx, CO, and hydrocarbons) and very low noise emissions. The major research issue in fuel cell technology is how to get the hydrogen to the vehicles. Production of hydrogen from gasoline through partial oxidation and steam reforming are the two most promising technologies, but reforming cannot be scaled down due to heat losses and the size of the furnace. It is an endothermic reaction, and coke formation is a potential problem. Catalytic partial oxidation has advantages over steam reforming; it is exothermic, and hasa short contact time. It is promising and this process was investigated numerically and experimentally in this work.

The objective of this work was to combine assumptions, good elements from previous models, time dependency and the energy equation to simulate catalytic partial oxidation of methane in a monolithic reactor for the production of synthesis gas. The data generated from this study can be used for the understanding of the treatment of heat transfer between the solid and gaseous phase, conduction of heat in the catalytic monolith, and mass transfer. This work offers insight into how the catalyst temperature develops in time and in space. Simulation results show that the improvement in syngas yields are due to improved temperature profiles. Although the predictions suffer from the limited accuracy of the applied kinetics.

The performed simulations illustrated time dependency, solved the energy equations, showed the concentration profile inside the monolith, and explained the effect of different hydrodynamic conditions in a monolithic reactor. The accuracy of the model is not as good as expected, but necessary improvements in the reaction kinetics can be made to improve the accuracy of the reactant conversions and product selectivities in the simulations.

List of Symbols

$A(k_i)$	pre-exponential factor of rate coefficient, k_i
$A(K_j)$	pre-exponential factor of adsorption constant, K_j
E_i	activation energy of reaction i, kJ/mol
ΔH	enthalpy change of reaction or adsorption, kJ/mol
R	gas constant
r_i	rate of reaction
T	temperature, Celsius
Q	heat generated
λ	thermal conductivity, W/m/K
S_i	selectivity of component i, %
K	equilibrium constant
k	forward rate constant
u	superficial gas velocity, m/s
X_i	conversion of component i, %
F_i	flow rate
ε	monolith void fraction
V	volume of the monolith
D_i	diffusion coefficient
c_i	concentration of component i, mol/m^3
η	viscosity,
c_p	heat capacity, J/mol/K
ρ	density, kg/m^3
ppi	pore per linear inch
z	reactor length, mm
t	time, s

List of Abbreviations

PEMFC	Proton exchange membranes fuel cell
PFTR	Plug flow tubular reactor
GHSV	Gas hour space velocity
MFC	Mass flow controller
TCD	Thermal conductivity detector
CPO	Catalytic partial oxidation
STP	Standard temperature and pression
CPU	Central Processing Unit
PDE	Partial differential equation

References

[1] D. Hickman, E. Haupfear, and L. Schmidt, "Steps in ch4 oxidation of pt and rh surfaces: High-temperature reactor simulations," *AIChE Journal*, vol. 39, p. 1164, 1993.

[2] P. Witt and L. Schmidt, "Effect of flow rate on the partial oxidation of methane and ethane," *Journal of Catalyst*, vol. 163, pp. 465–475, 1996.

[3] O. Deutschmann and L. D. Schmidt, "Modeling the partial oxidation of methane in a short-contact-time reactor," *AIChE Journal*, vol. 44, pp. 2465–2477, 1998.

[4] A. S. Bodke, S. S. Bharadwaj, and L. D. Schmidt, "The effect of ceramic supports on partial oxidation of hydrocarbons over noble metal coated monoliths," *Journal of Catalyst*, vol. 179, pp. 138–149, 1998.

[5] A. D. III and L.D.Schmidt, "Effect of pressure on three catalytic partial oxidation reactions at millisecond contact times," *Catalysis Letters*, vol. 33, pp. 223–237, 1993.

[6] R. Schwiedernoch, S. Tischer, H.-R. Volpp, and O. Deutschmann, "Towards a better understanding of transient processes in catalytic oxidation reactors," *Natural Gas Conversion VII, Studies in Surface Science and Catalysis*, vol. 147, pp. 511–516, 2004.

[7] C. 3.2

[8] P. Torniainen, X. Chu, and L. Schmidt, "Comparison of monolith supported metals for the direct oxidation of methane to syngas," *Journal of Catalysis*, vol. 146, pp. 1–10, 1994.

[9] G. Tong, J. Flynn, and C. Leclerc, "A dual bed for the autothermal partial oxidation of methane to synthesis gas," *Catalysis Letters*, vol. 102, pp. 131–137, 2005.

[10] L. Ma, D. Trimm, and C. Jiang, "The design and testing of an autothermal reactor for the conversion of light hydrocarbons to hydrogen i. the kinetics of

the catalytic oxidation of light hydrocarbons," *Applied Catalysis A:General*, vol. 138, pp. 275–283, 1996.

[11] J. Xu and G. F. Froment, "Methane steam reforming, methanation and water-gas shift:i. intrinsic kinectics," *AIChE Journal*, vol. 35, pp. 88–96, 1989.

[12] U. Olsbye, T. Wurzel, and L. Mleczko, "Kinetic and reaction engineering studies of dry reforming of methane over a ni/la/al_2o_3 catalyst," *Ind. Eng. Chem. Res.*, vol. 36, pp. 5180–5188, 1997.

[13] K. Williams, C. Leclerc, and L. Schmidt, "Rapid lightoff of syngas production from methane: A transient product analysis," *AIChE Journal*, vol. 51, p. 247, 2005.

[14] L. Ma and D. Trimm, "Alternative catalyst bed configurations for the autothermic conversion of methane to hydrogen," *Applied Catalysis A:General*, vol. 138, pp. 265–273, 1996.

[15] S. R., S. Tischer, C. Correa, and O. Deutschmann, "Experimental and numerical study on the transient behavior of partial oxidation of methane in a catalytic monolith," *Chemical Engineering Science*, vol. 58, pp. 633–642, 2003.